Phonon spectral densities of Cu surfaces: Application to Cu(211)

M-C. Mărinică and G. Raşeev*
Laboratoire de Photophysique Moléculaire du Centre National de La Recherche Scientifique, Bâtiment 210, Université Paris-Sud, 91405 Orsay Cedex, France

K. S. Smirnov
Laboratoire de Spectrochimie Infrarouge et Raman, Bâtiment C5, Université des Sciences et Technologies de Lille, 59655 Villeneuve d'Ascq Cedex, France

(Received 15 December 2000; published 4 May 2001)

Power phonon spectra of vicinal stepped surfaces of Cu(211) have been calculated using a molecular dynamics method combined with a semiempirical potential. The potential is based on an analytic form of inverse powers proposed by Finnis and Sinclair with the parametrization of Sutton and Chen. One of the four independent parameters of the potential was rescaled to reproduce the bulk phonon spectrum of Cu while retaining other properties of the bulk Cu close to the experimental values. Using this potential, we calculated the power surface phonon spectra, projection of the spectra at the high-symmetry points of surface Brillouin zone (SBZ), and the mean square displacements (MSD's) of atoms of the Cu(211) surface. The calculated projected phonon spectra at $\bar{\Gamma}$ and at two new SBZ points (at $\bar{X}$ and $\bar{Y}$) compare favorably with experiment and theory when available. The MSD of the Cu(211) surface is also well reproduced and its temperature dependence shows that anharmonicity of the atomic motion becomes important above 200 K.

DOI: 10.1103/PhysRevB.63.205422 PACS number(s): 68.35.Ja, 63.20.−e, 78.30.−j

I. INTRODUCTION

Stepped vicinal surfaces consisting of ordered arrays of atomic steps separated by low-index terraces represent good models for the real surfaces, which play an important role in catalysis, nucleation, and crystal growth. For the real surfaces the structural defects reproduced on the vicinal surfaces by steps are often found to be preferred for adsorption of atoms and molecules and can be sites of chemical activity. At certain conditions, these defects can cause either acceleration or retardation of a process taking place at surface, for example, a chemical reaction. Understanding of surface phenomena often necessitates information about the microscopic energy transfer on surfaces and thus requires a detailed knowledge about surface phonon spectra and dynamics of surface atoms.

The phonon spectra of stepped surfaces have been studied by modern experimental surface science techniques. Witte *et al.*[1] and Niu *et al.*[2] used the helium atom scattering method (HAS) to obtain the phonon dispersion curves for Cu(211), Cu(511), and Ni(977) surfaces for phonons with frequencies below 130 cm^{-1}. Recently, results of the experimental study of phonon spectrum in different symmetry points of surface Brillouin zone (SBZ) using high-resolution electron energy loss spectroscopy (HREELS) have been reported by Kara *et al.*[3] for Cu(211), Cu(511), and Cu(331) surfaces. For stepped surfaces with (100) step facet the authors of Ref. 3 gave evidence of a vibrational mode with a frequency at the center of SBZ above the bulk cut-off band.

A widely used model for theoretical description of a surface is the slab model[4–6] where the solid-gas interface is represented as two terminal surfaces of a slab formed by a sequence of atomic layers. Various theoretical methods employ the slab model to calculate the phonon spectrum and phonon dispersion curves of surfaces. Some of these methods make use of the harmonic approximation (HA), and others do not. Thus, in one of such HA method the phonon frequencies are obtained via diagonalization of a dynamical matrix (DM), a matrix of second derivatives of the potential energy with respect to the atomic displacements. Eigenvalues of the dynamical matrix, obtained at each allowed point of the SBZ, serve to construct phonon dispersion curves, whereas the corresponding eigenvectors permit us to identify the atomic motions associated with a particular vibrational mode. The necessary dynamical matrix can be obtained in different ways. Particularly, harmonic potentials can be used to construct such a dynamical matrix, the dynamical-matrix force constant (DM FC). These force constants are fitted from the experimental elastic constants and bulk or/and surface phonon frequencies, or computed directly from semiempirical and *ab initio* calculations. Studies of the phonon spectra of stepped surfaces using the DM method with the harmonic effective potentials have been performed for unrelaxed stepped nickel surfaces by Armand and Masri,[7] Black and Bopp,[8] and Knipp.[9] *Ab initio* calculations have been performed for Cu(211) surfaces at $\bar{\Gamma}$ point of the SBZ by Wei *et al.*[10] The authors used DM-FC method to obtain the vibrational spectrum and revealed vibrational modes that cannot be seen by the HAS experiment. Sklyadneva *et al.*[11] used the DM method together with an embedded-atom potential model (EAM) to calculate the vibrational spectra for relaxed stepped surfaces of Ag, Cu, Al, and Pd.

Another HA method, where the surface is treated as a perturbation of the bulk lattice, uses the Green function (GF) perturbational approach. This method gives information about surface phonon density of states and permits a clear discrimination between surface localized modes and surface resonances. Using the GF method Durukanogulu and co-workers[12,13] calculated the local vibrational densities of states for (211), (511), and (331) surfaces of Cu. Tian and Black[14] studied the local density of phonons for Cu(11n)

surfaces using an EAM potential and the GF-HA method coupled with the continued fraction solution for the matrix inversion. In addition to the phonon frequencies, the GF technique yields mean-square displacements (MSD's) of atoms, surface specific heats, and other thermodynamic observables.

A method based on the slab model that has not been used as extensively for the calculations of surface phonons is the MD technique. In the MD method the atomic dynamics evolves according to laws of classical mechanics and the phonon spectrum is obtained as Fourier transformation of the autocorrelation function of velocity of atoms.[15–17] The calculations are not limited by the harmonic approximation and they permit us to study the influence of temperature on the spectrum.[18–23] The MD simulations have been used by Lynden-Bell and co-workers[24–26] in their studies of the roughening transition, relaxation at stepped surfaces, and migration of adatoms on such surfaces. The authors employed a many-body potential proposed by Sutton and Chen[27] (SC) based on the analytic form of Finnis and Sinclair.[28] Using the MD method and the same potential, Koleske and Sibener[21] (KS) calculated the surface phonon spectral densities for basal planes of Ni and Cu metals.

In this paper we use the MD method to calculate the phonon spectra and to identify surface and resonance vibrational states of the stepped (211) surface of Cu. To achieve this aim we have rescaled the SC potential[28,27] in such a way to fit the phonon spectra of bulk Cu metal. We show that this rescaled potential (RSC) gives excellent agreement between the calculated phonon spectrum of the flat (100) and (111) and stepped (211) surfaces and the experiment. Particularly for the (211) surface we obtain an agreement with the spectra obtained by Witte *et al.*[1] using HAS and by Kara *et al.*[3] using HREELS experiments. We then compute the temperature dependence of the theoretical phonon spectrum and the MSD of atoms up to temperature of 450 K. Results of the calculations are compared with data obtained by Durukanogulu and co-workers[12,13] using the GF method in the HA approximation.

The paper is organized as follows. In the next section we present the computational approach and provide some details of the calculation. To verify the validity of the rescaled SC potential detailed in the Appendix, the third section first briefly discusses the phonon spectra computed with the RSC potential for Cu(100) and Cu(111) surfaces. A subsequent part of this section is devoted to the results about the phonon spectra (local and projected in SBZ) of the Cu(211) surface, the MSD and dependences of these characteristics on the system temperature. The fourth section discusses the results obtained and presents the conclusions.

II. MODEL

A reasonable physical model to study the dynamics of metallic surfaces consists of atoms interacting through an effective interatomic potential optimized so that they mimic as closely as possible an observable, here the vibrational spectrum of the bulk. The MD method then provides algorithms to solve the Hamilton equations of motion of the classical dynamics for the system atoms interacting via the potential. We start this section by presenting a way used to calculate the vibrational properties from an MD simulation. We then describe the SC and RSC potentials and end with computational details.

A. Molecular dynamics and vibrational spectra

In a MD simulation the coordinates and velocities of the atoms are computed in a step-by-step procedure for a sufficiently long period of time, and thus a trajectory of the system in the phase space is obtained. Assuming ergodicity of the system, its characteristics are then extracted by averaging their instantaneous values along the trajectory. Particularly, the vibrational dynamics can be expressed through the power spectrum $S(\nu)$ obtained by the Fourier transform of the velocity $\vec{v}_j(t)$ autocorrelation function:

$$S(\nu)=\sum_{\alpha=x,y,z} S_\alpha(\nu) \propto \sum_{\alpha=x,y,z}\sum_{j=1}^{N}\int_0^\infty e^{2i\pi\nu t}\langle v_{j\alpha}(t)v_{j\alpha}(0)\rangle dt, \qquad (1)$$

where $v_{j\alpha}$ is the component of the velocity of the jth atom in the direction α ($\alpha=x,y,z$ denotes the Cartesian axes). If one wants to obtain the spectrum of a particular set of atoms, the sum in Eq. (1) is restricted to that set of atoms and polarization. Hereafter this quantity is called a local spectral density of phonons (LSDP).

LSPD of a surface layer computed via Eq. (1) contains contributions to the $S(\nu)$ from all allowed points (and their transferred momentum) of the SBZ. The local spectral density of phonons in a particular $\vec{K}$ point of the SBZ is obtained from the layer-averaged velocity for this point given by the following equation:[16,17,19–22,29]

$$V_\alpha(\vec{K},t)=\sum_{j\in\text{layer}} v_{j\alpha}(t)e^{i\vec{K}\cdot\vec{r}_j(t)}, \qquad (2)$$

where $\vec{K}\cdot\vec{r}_j(t)$ denotes the inner product between the two-dimensional vector $\vec{K}$ of the SBZ and the position $\vec{r}_j(t)$ of jth atom. A projected local spectral density of phonons (PLSDP) is then computed by the Fourier transform of the autocorrelation function of the velocity (2):

$$S_\alpha(\nu,\vec{K})\propto\int_0^\infty e^{2i\pi\nu t}\langle V_\alpha(\vec{K},t)V_\alpha(-\vec{K},0)\rangle dt = \int_0^\infty e^{2i\pi\nu t}\left\langle\left[\sum_j e^{i\vec{K}\cdot\vec{r}_j(t)}v_{j\alpha}(t)\right]\times\left[\sum_j e^{-i\vec{K}\cdot\vec{r}_j(0)}v_{j\alpha}(0)\right]\right\rangle dt. \qquad (3)$$

The calculation of PLSDP is described in detail in Refs. 16, 30, 19, and 23. To evaluate $S(\nu)$ and $S_\alpha(\nu,\vec{K})$ one does not need to calculate the autocorrelation functions explicitly. Instead, one can take advantage of the Wigner-Khinchin

theorem[31] and compute the spectra via the Fourier transform (FT) of the time history of the $v_{j\alpha}(t)$ and $V_\alpha(\vec{K},t)$ quantities. From the physical point of view, PLSDP defined by Eq. (3) is proportional to an observable corresponding to the phonon excitation process due to, e.g., a particle collision with the surface with a momentum transfer $\vec{K}$ to or from the surface. In the next sections we will also calculate LSDP $S^I_\alpha(\nu)$ and PLSDP $S^I_\alpha(\nu,\vec{K})$, where I denotes the index of the Ith layer of the slab. The larger the value of I, the more deeply the layer is situated, and the maximum value of I corresponds to the bulk. Such a calculation of the power spectra in the layer-by-layer manner allows us to discriminate between surface and bulk vibrational states and resonances. Respectively, these states are localized at the surface, in the bulk, or result from an interaction of the surface and bulk states.

Regardless of the effective interatomic potential used in the MD simulations, the anharmonicity is inherently included in the calculated spectra because no harmonic approximation is made in the formulation presented above. However, it is worth noticing that in the classical MD method, the temperature is defined through the classical kinetic energy of the system. To include the quantum zero-point motion contribution that is important at low temperatures we follow the work of Wang *et al.*[30] and adopt a simple rescaling procedure of the temperature of the system. In particular, for the Cu system a rescaling coefficient for the temperature is taken from Fig. 10 of the work of Tian and Black.[14]

The statistical noise of the peak intensities in the computed spectra depends on both the number of particles used in the spectra calculation and on the number of points in the time history of the $v_{j\alpha}(t)$ and $V_\alpha(\vec{K},t)$ quantities. Having fixed the number of atoms N the noise can therefore be reduced by either taking one long trajectory or several short trajectories subsequently averaged. The last method seems to be preferable because (i) the use of the different initial conditions in the MD simulations at a given temperature allows one to sample a larger portion of the phase space and (ii) the energy conservation criterion is better obeyed for a short trajectory. Thus, having obtained a set of power spectra derived from n independent trajectories $\mathcal{T}_1, \mathcal{T}_2, \ldots, \mathcal{T}_n$ the resulting power spectrum is then given as the following average:

$$S(\nu)=\frac{1}{n}\sum_{i=1}^{n} S^{\mathcal{T}_i}(\nu), \tag{4}$$

resulting from an insufficient number of averages and the finite length of the MD trajectories, and the LSDP given by Eq. (4) is convoluted with a Gaussian function of a width 7 cm^{-1}. This width has a typical experimental resolution of 2–8 cm^{-1} in HAS and HREELS experiments.[1,3] Note that the published theoretical results have also been obtained with the use of such a convolution procedure for the spectra.[12–14] For PLSDP we do not perform such a convolution because we are interested in peak positions only.

B. Sutton-Chen potential

A widely used physical model for the study of the dynamics of metallic systems consists of ions placed in a sea of free outer electrons. The ions, being the nuclei plus inner electrons, interact with the outer electrons via an effective potential. If the potential is semiempirical, as in the present study, the clue is to optimize its parameters so that it matches, as closely as possible, a wide range observables.

Finnis and Sinclair[28] (FS) have proposed an analytic form of the interatomic potential appropriate for transition metals having nearly filled d shells, such as Ni and Cu. This potential is based on the second-moment approximation to the tight binding (TB) model, where the binding energy per atom varies as the square root of the atomic coordination. For these metals in general, and for Cu in particular, Sutton and Chen (SC) have suggested a semiempirical parametrization based on the FS functional form.[27] In the SC potential the energy of atoms embedded in a ''sea'' of electrons of a local density ρ_i is written as

$$U=\sum_i \epsilon\left[\frac{1}{2}\sum_{j\neq i}\left(\frac{a}{r_{ij}}\right)^n - c\sqrt{\rho_i}\right], \tag{5}$$

where the local density of the electrons is represented as

$$\rho_i=\sum_{j\neq i}\left(\frac{a}{r_{ij}}\right)^m \tag{6}$$

and r_{ij} signifies distance between atoms i and j. The first term in Eq. (5) accounts for the repulsion between the ions, whereas the second term stands for the attraction energy due to the ion–outer-electron interactions. According to Sutton and Chen,[27] only two of three parameters a, c, and ϵ of the potential are independent, namely, ϵ scales the energy and a the lattice spacing. The choice of n determines the steepness of the repulsive potential, whereas m determines it for the attractive interactions. The total number of meaningful parameters of the potential is therefore equal to four. Despite the many-body character of the second term of Eq. (5), the potential energy and the force on each atom can be written as a sum of pairwise contributions.[28] The SC potential can be interpreted as being similar to the EAM potential.[32]

Requiring integer n and m with $n>m$ and fixing the cohesion energy, Sutton and Chen[27] have fitted the parameters of Eqs. (5) and (6) to the elastic bulk constants of a particular metal. For Cu metal the retained values for the exponents n and m are 9 and 6, respectively. The results of the previous computational studies[24–26,21] showed that the SC potential is adequate for the qualitative and semiquantitative description of the structure and dynamics of flat surfaces of transition metals.

Compared to the experimental data,[33–36] our preliminary results obtained with the FS-SC potential revealed a general downward shift of bands in the phonon spectra for the bulk and for flat (100) and (111) surfaces. Instead of modifying the FS-SC potential, one can use a different analytic form. Using Ni bulk and surface characteristics as a reference, KS made a detailed comparison between potentials constructed with the inverse power (FS-SC) functional based on four

TABLE I. Experimental and calculated positions (in cm^{-1}) of two selected peaks in the bulk phonon spectrum of Cu.

Frequency	Expt. [a]	Ref. 13	Ref. 14	SC [b]	RSC
ν_L	224	305	230	204	223
ν_T	163	145	150	135	155

[a]Reference 46.
[b]Reference 27.

independent parameters and the original EAM based on a large number of parameters. In general, the EAM potential yields the bulk and surface spectra that compare favorably with the experiment, whereas the spectra obtained with the FS-SC potential are displaced to lower wave numbers. This feature was related by KS to a nonexplicit calculation of the second-order changes in the *d*-band structure in FS-SC model. In the present work no electronic calculations were performed and therefore we cannot discuss this point directly. Levanov *et al.*[37] used a potential with the same number of parameters as FS and SC, where the inverse power functional form is replaced by an exponential form. We tried to use this exponential form and found that, because of a faster decay with the atom-atom distance than the inverse power form, the resulting phonon spectrum can give frequencies not higher than 160 cm^{-1}.

In the present work we keep the inverse power functional form of the potential and, to obtain a quantitative agreement between the experiment and calculations, we rescale the FS-SC potential by fitting to the experiment the phonon spectrum and elastic constants of the *bulk* Cu. The details of the rescaling procedure and the performed tests for the bulk Cu metal are given in the Appendix. Using the RSC, two selected vibrational frequencies in the bulk Cu power spectrum, the longitudinal mode (ν_L) at 163 cm^{-1} and the transversal mode (ν_T) at 224 cm^{-1}, are calculated close to the experiment and to the other theoretical results (see Table I). However, the RSC potential gives a cohesive energy E_{coh} 10% above the experimental value, while the elastic constants remain in the range of the experimental values (see Table II for a detailed comparison). The above energetic difference should play a marginal role for the properties of interest where what matters is the local shape of the potential but not the absolute value of energy at the potential minimum.

TABLE II. Comparison of the cohesive energy and elastic constants (units are eV $Å^{-1}$) for bulk Cu computed using the SC and RSC potentials.

Calc.	E_{coh} (eV)	c_{11}	c_{12}	c_{44}
Experience [a]	3.50	1.10	0.78	0.51
SC [b]	3.50	1.06	0.81	0.36
RSC (present)	3.80	1.14	0.87	0.39

[a]Reference 47.
[b]Reference 27.

C. Computational details

The size and shape of the system used in the MD simulations are described in the corresponding sections of the paper in detail (vide infra). The calculations were carried out with periodic boundary conditions and the minimum image convention[38] applied to system in three and two directions for the bulk and surfaces simulations, respectively. Following Ref. 39 the thermal expansion of the Cu crystal was taken into account by defining the temperature-dependent lattice nearest-neighbor distance $a_{\mathrm{NN}}=a^0_{\mathrm{NN}}\exp[1.2\times10^{-5}T]$, where $a^0_{\mathrm{NN}}=2.552\,66$ Å and T is the temperature of the system in kelvins. The a_{NN} distance was then used to obtain the parameters of the MD box employed in the simulations. A cutoff radius of $3.5a_{\mathrm{NN}}$ for the interatomic potential[24–26] was employed.

The classical equations of motion were integrated with the use of the velocity form of Verlet algorithm with time step of 0.8 fs. The $S(\nu)$ spectrum in Eq. (4) was obtained as an average of 30 independent trajectories $\mathcal{T}_i$. Each of the trajectories $\mathcal{T}_i$ was calculated starting from the randomly chosen atomic velocities corresponding to a Maxwell distribution at the desired temperature. The system was then equilibrated at the temperature T by coupling to a temperature bath[40] during 50–80 ps. The equilibration stage was longer for stepped surfaces than that for flat surfaces or bulk. This procedure ensures that the bulk or surface relaxation process has been completed and the system is in thermodynamical equilibrium at the desired temperature. After the equilibration, the simulation was continued in the microcanonical (NVE) ensemble for 132 ps and the positions $[\vec{r}_{j\alpha}(t)]$ and velocities $[\vec{v}_{j\alpha}(t)]$ of the atoms were stored for a subsequent analysis. During the NVE stage of the calculations, the drift of the total energy from its initial value was less than 10^{-4}%, and the ratio $\sigma(E_{\mathrm{tot}})/\sigma(E_{\mathrm{kinetic}})$ of the root mean square fluctuations of the total and kinetic energies was less than 2%.

III. RESULTS

In this section we present the LSDP, PLSDP, and MSD's of the atoms for flat and stepped (211) surfaces of Cu. We have also calculated a variation of LSDP and MSD with the temperature. Detailed studies concerning the relaxation of surface layers and the energetics of the step-step interaction on these surfaces have been published by the group of Lynden-Bell and co-workers.[24–26] We have obtained similar results for this relaxation and we will omit the related discussion in the following sections.

A. Phonon spectra of flat Cu(100) and Cu(111) surfaces

To test the RSC potential for the properties of a surface, we have computed the LSDP and PLSDP for the flat Cu(100) and Cu(111) surfaces. In the calculations, the slab was composed of 27 atomic layers each built from 8 atoms (or elementary cells) in every crystallographic direction parallel to the surface, totally 1728 atoms. All the atoms were allowed to move and consequently each effective layer used in the spectra calculations is composed of two layers that are equivalent with respect to the middle layer of the slab. The

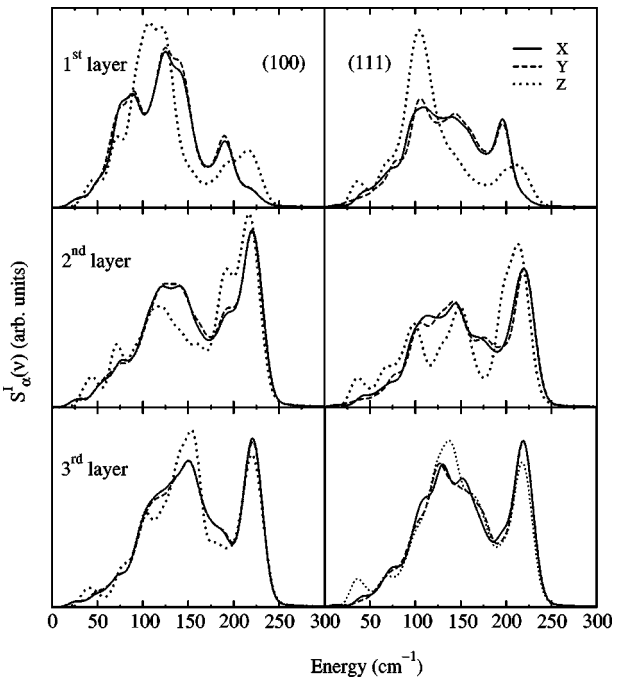

FIG. 1. Local spectral density of phonons (LSDP) at the temperature of 150 K for the first three layers of Cu(100) (left) and Cu(111) (right) surfaces in three directions X ([100] respective $[\bar{1}10]$), Y ([010] respective $[11\bar{1}]$), and Z ([100] respective [111]).

present system permits calculation of 81 and 73 points in the SBZ for the (100) and (111) surfaces, respectively. The Z axis of the Cartesian frame was chosen to be normal to the surfaces. In the direct space the X axis corresponds to [100] and $[\bar{1}10]$ crystallographic directions for Cu(100) and Cu(111) surfaces, respectively. In the reciprocal space this axis is defined by the $\overline{\Gamma X}$ direction. The Y axis corresponds in the direct space to the [010] and $[11\bar{1}]$ directions for Cu(100) and Cu(111), respectively. In the reciprocal space the Y axis is given by $\overline{\Gamma X}$ and $\overline{\Gamma M}$ directions for the (100) and (111) surfaces, respectively.

Figure 1 displays the LSDP calculated at the temperature of 150 K for the first three layers of Cu(100) and Cu(111) surfaces. The LSDP of the first layer in the Z direction (or for Z polarization) has sharp peaks at 111 cm^{-1} and 105 cm^{-1} for the (111) and also (100) surfaces, respectively. The peaks diminish in the second and disappear in the third layer. A high-frequency band located at 190 cm^{-1} for (100) and at 197 cm^{-1} for (111) surfaces in the first layer and X and Y directions reveals a monotonic upward shift while going from the first layer toward the bulk. In the spectra of the second layer this band is calculated to be at about 215 cm^{-1} for both surfaces and it converges to the bulk frequency ν_L at 223 cm^{-1} in the spectra of the third layer. Small differences between the LSDP in X and Y directions for the (111) surface are due to the fact that these two directions are not equivalent in the reciprocal space. Note that in Z direction, the high-frequency edge of the spectrum is less sensitive to the presence of the surface. The calculated spectra are in an excellent agreement with the work of Tian and Black,[14] who used an EAM potential and the Green function formulation in harmonic approximation.

TABLE III. Phonon modes frequency (in cm^{-1}) in selected points of SBZ for Cu(100) and Cu(111) surfaces. The labeling follows the established nomenclature (Refs. 4–6). The experimental data are taken from Refs. 33 and 34 and from Refs. 35 and 36 for Cu(100) and Cu(111) surfaces, respectively.

$\bar{K}$ Point	Polarization	Layer	Mode	KS [a]	Present	Expt.
			Cu(100)			
$\bar{X}$	Z	1	S_4	85.4	101	108.1±1.61
$\bar{M}$	Z	1	S_1	113.7	126	133.8±2.41
			Cu(111)			
$\bar{M}$	Z	1,2	S_1	84.6	106	104.8±1.61
	Z	2	R_1	133.0	150	147.5±4.83
	X	1	S_2	172.6	195	205.6±1.61
	X	2	R_2	200.8	225	228.2±1.61

[a]Reference 21.

Using Eq. (3) we evaluate the PLSDP for a selected set of points of the SBZ. Table III gathers the results of the calculations and compares them with the results of calculations by KS and the experimental data for Cu(100) (Refs. 33 and 34) and for Cu(111) (Refs. 35 and 36) surfaces. The agreement between the present results and the experimental data is much better than that in the simulations done by KS. This improvement is directly related to the RSC potential optimized to reproduce the bulk properties. The present test calculations of the flat Cu surfaces with the RSC potential showed that this potential is suitable for the calculation of the surface phonon spectra. We will now proceed with the calculation of the vibrational spectra of the stepped Cu(211) surface.

B. Stepped Cu(211) surface

The stepped (211) surface of a fcc crystal is built from (100) steps of two rows and (111) terraces of three rows (Fig. 2). We have chosen the surface plane with the X coordinate along $[01\bar{1}]$ parallel to the step-edge atoms and Y coordinate

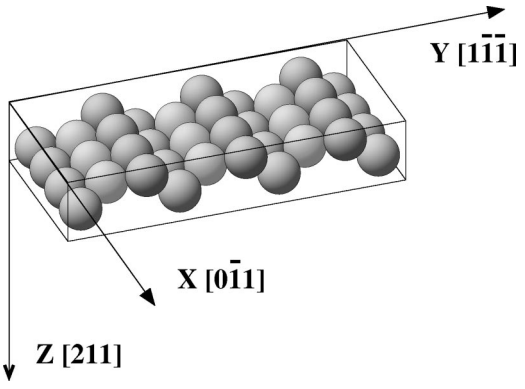

FIG. 2. Coordinate system used in the MD simulations of the (211) surface of Cu.

along $[1\bar{1}\bar{1}]$ perpendicular to the steps. By definition of the surface cut the Z direction is along [211] perpendicular to the surface (Fig. 2). It can be demonstrated that on $(n11)$ surfaces with $n=$even, the angle between the [111] direction and $[n11]$ is $\arcsin[\sqrt{2/3}(2+n^2)^{-1/2}]$ [19.5° for (211) surface] and the spacing between $(n11)$ planes is $a_{\mathrm{NN}}(2+n^2)^{-1/2}$. It follows that, regarding X and Y directions, the first and seventh layers are equivalent. In our MD calculations we use 6 and 4 atoms in X and Y directions, yielding 35 allowed points in the SBZ of the Cu(211) surface, and we take a slab composed by 72 layers.

Figure 3 presents the LSDP calculated for the Cu(211) surface. The spectrum of the first layer (step-edge-atom chain, SC) in the Y direction perpendicular to the steps displays a soft mode at 83 cm^{-1} due to the loss of the nearest neighbors at the step edge (see Fig. 2). This mode is also present in the spectra computed with the Green function method.[12,9] In the X direction parallel to the steps and in the Z direction perpendicular to the surface the spectra are similar to the corresponding LSDP of the first layer of the Cu(100) surface. Thus, the X- and Z-polarized spectra of the (211) surface reveal two peaks at 123 cm^{-1} and 124 cm^{-1}, appearing in inverted order on the Cu(100) surface (see Fig. 1). In addition, above 200 cm^{-1} the Z-polarized spectra present a high-frequency peak at 213 cm^{-1} and 228 cm^{-1}, respectively, for the (100) and (211) surfaces.

The spectrum of the second layer (terrace-atom chain, TC; see Fig. 3) in the Z direction displays a pronounced peak at 100 cm^{-1}, which is similar in position and shape to a Z polarized peak in the first atomic layer of (111) surface (see Fig. 1). For the TC layer, high-frequency vibrations with X and Y polarization are shifted downward to 200 and 178 cm^{-1}, respectively, from an unique mode at 223 cm^{-1} on the (111) surface. For the third atomic layer (corner step-terrace-atom chain, CC) these vibrations appear at 200 and 210 cm^{-1} for X and Y directions, respectively. For TC and CC layers of the stepped (211) surface the frequency of the X-polarized vibration remains unchanged at 200 cm^{-1}, whereas the frequency of the Y-polarized vibration in the CC layer is shifted upwards by 32 cm^{-1}. This shows that atoms of the TC layer are less bound in the Y direction than in the CC layer, with no difference in the X direction. This behavior will further be compared with the mean square atomic displacements in the layers (vide infra).

The above comparison of power spectra of flat and stepped surfaces reveals similarities between the SC and TC layers and, respectively, the (100) and (111) surfaces. Thus, the spectra reflect chain and local orders along and perpendicular to the step. The analysis of Fig. 3 also reveals the presence of localized modes: one with Y polarization in the first layer at 83 cm^{-1} and the other with Z polarization in the second layer at 100 cm^{-1}.

The temperature dependence of the LSDP spectrum and MSD for (211) stepped surfaces reveals the different environments of the surface atoms. In Fig. 4 we present the LSDP spectrum of the first layer of Cu(211) surface in the Y direction (perpendicular to the steps), where the spectrum variations with an increase of the temperature are clearly

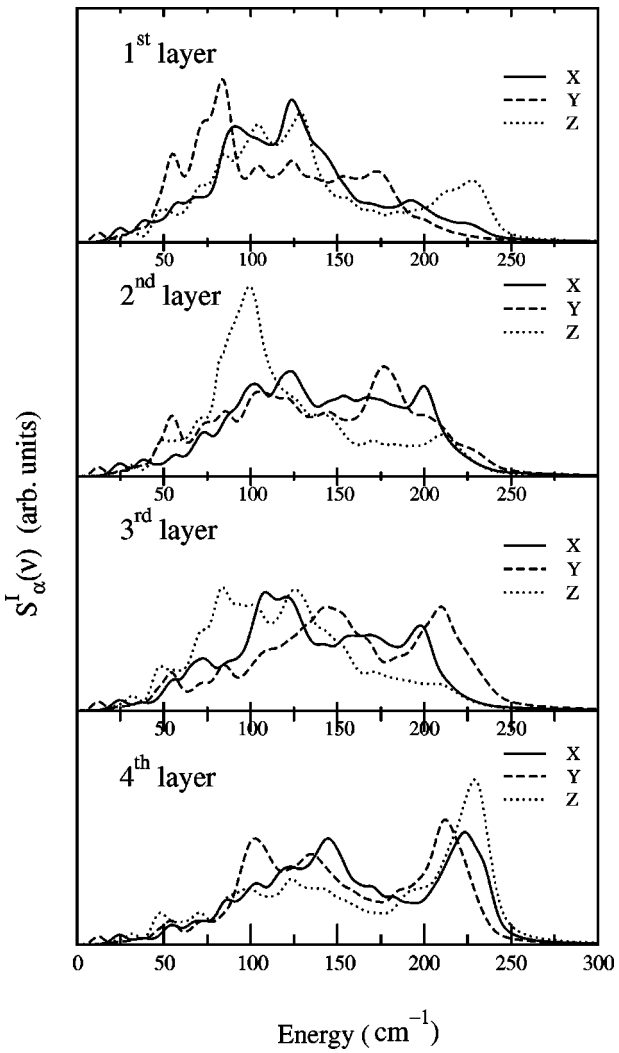

FIG. 3. LSDP at the temperature of 150 K for the first four layers of the Cu(211) surface in three directions X ($[01\bar{1}]$), Y ($[1\bar{1}\bar{1}]$), and Z ([211]). The first layer corresponds to the step-edge atom chain (SC), the second layer to the terrace-atom chain (TC), and the third to the corner step terrace-atom chain (CC).

identified. As a general trend the temperature dependence of the spectrum is weak and it is mainly due to the anharmonicity of the potential that becomes more pronounced with the increase of temperature (vibrational amplitudes). More specifically, going from 100 to 450 K there is a downward shift of 8 cm^{-1} in the region above 100 cm^{-1} and of 4–5 cm^{-1} for the low-energy edge of the spectrum. When the temperature rises a shoulder at 75 cm^{-1} disappears and the relative peak intensity is slightly changed (for example, the peak at 105 cm^{-1} relative to the peak at 125 cm^{-1}). Note also a broadening of the peaks in the spectra.

To establish a qualitative relation between the phonon spectrum and the MSD we assume that at low temperature the system can be described as an ensemble of harmonic oscillators (normal modes). The Cartesian atomic displacements are then a linear combination of the normal modes of the system and the MSD in a direction α depends on the distribution of the normal modes in the spectrum of the at-

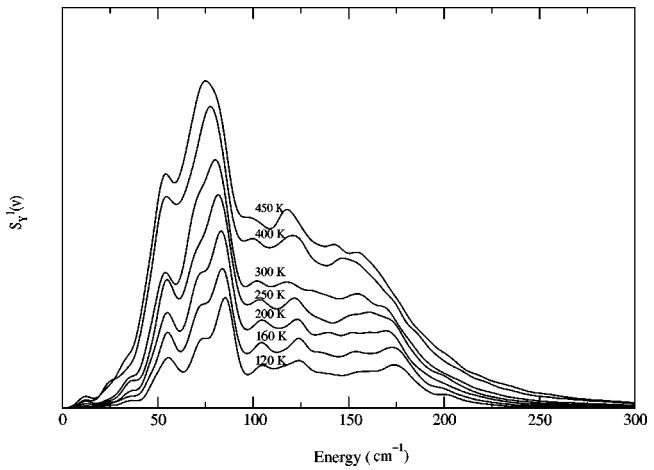

FIG. 4. LSDP of the first layer (CC) in the Y ($[1\bar{1}\bar{1}]$) direction perpendicular to the step edges for several temperatures between 120 and 450 K.

oms $S_\alpha(\nu)$. It is straightforward to show that an effective amplitude A of a normal mode with frequency, ν is

$$A^2 = \frac{k_B T}{4\pi^2 \nu^2 \mu}, \tag{7}$$

where μ is an effective mass of the oscillator. The above equation shows that the vibrational amplitude is inversely proportional to mode's frequency, and particularly, one might expect that the atoms with an intense low-frequency part of the spectrum have larger vibrational amplitudes.

Let us analyze the LSDP displayed in Fig. 3 from this viewpoint and compare it with MSD displayed in Fig. 5. As expected from the environment of the atoms, the MSD's diminish from SC to TC and to CC atoms in X and Y directions. The Y-polarized spectrum of the SC atoms has an intense low-frequency part (Fig. 3), in line with a large MSD calculated in this direction (see $\langle \Delta r_y^2 \rangle$ graph in Fig. 5). A Similar analysis performed for the Y-polarized LSDP of the TC and CC atoms shows that the MSD of the former atoms is larger than that of the latter, again in line with LSDP displaced to higher frequencies for CC atoms. Now in the X direction (see $\langle \Delta r_x^2 \rangle$ graph in Fig. 5) the spectral densities of phonons for the CC and TC atoms are similar, in an agreement with similar MSD's. Note that such an analysis has a qualitative character because for a quantitative description one should know, the spectral density of phonons (normal modes), the effective mass μ of each oscillator, and a coefficient that a particular normal mode contributes to the Cartesian displacement.

In Fig. 5 we also compare the MSD's obtained in the present MD simulations using the RSC potential with results calculated using GF-HA method by Rahman *et al.*[13] Schommers[41] established that for Lenard-Jones solids the anharmonic contributions to MSD become important at temperatures above $\frac{1}{3}T_{\text{melting}}$ and $\frac{1}{6}T_{\text{melting}}$ for bulk and flat surfaces, respectively. Figure 5 shows that differences between the data of MD simulations and those obtained in HA become significant at 150 K for MSD_Y^{SC}, 250 K for $\text{MSD}_Y^{\text{TC,CC}}$, 250 K for MSD_X^{SC}, and 300 K $\text{MSD}_X^{\text{TC,CC}}$. This indicates that

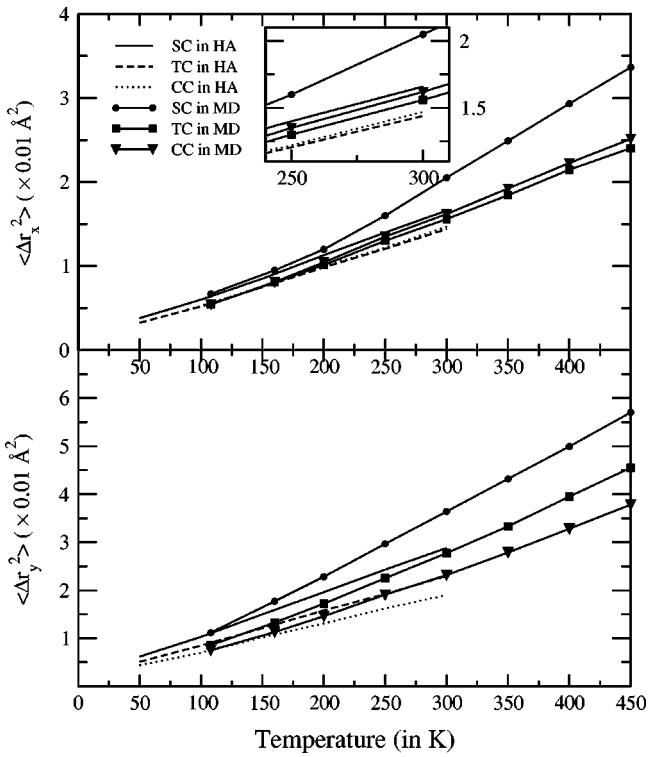

FIG. 5. Temperature dependence of the MSD's of atoms in the first layer (SC), in the second layer (TC), and in the third layer (CC). MD and HA refer to the results obtained in the MD simulations and by GF-HA method (Ref. 13), respectively.

for a stepped surface there is no unique temperature, e.g., for the SC atoms in the Y direction the anharmonicity plays an important role already at $T = \frac{1}{8}T_{\text{melting}}$ [taking $T_{\text{melting}} = 1350$ K for Cu (Ref. 42)]. For Cu(211) the present calculations reveal that the difference between the results of the finite-amplitude MD simulations and those obtained in the HA becomes globally important at $\frac{1}{5}T_{\text{melting}}$. The calculated higher temperature for the (211) surface is related to the many-body potential that stiffens the interaction for atoms on a stepped surface. We relate this stiffening to the lower coordination of stepped surfaces as compared to the flat surface atoms.

Let us now discuss the PLSDP at 250 K for a selected points of the surface Brillouin zone, namely for $\bar{X}$, $\bar{Y}$, and $\bar{\Gamma}$ points. For frequencies below 130 cm^{-1}, the calculated spectra are compared with HAS experiments of Witte *et al.*[1] and for higher frequencies with the HREELS experiments of Kara *et al.*[3] Note that $\bar{X}$ and $\bar{Y}$ points of the SBZ in the HAS spectra were obtained by extrapolating data from neighboring reciprocal space points.

In Fig. 6 we display the PLSDP computed for the first four surface layers and for the bulk projection at the $\bar{X}$ point of the reciprocal space. Note that the bulk projection spectrum in Fig. 6(e) corresponds to $S_\alpha^{36}(\nu, \bar{X})$, i.e., the PLSDP of the middle (36th) layer of the slab. For this bulk projection the three polarizations are identical and a single spectrum is therefore displayed. The low-frequency part of our calculated spectrum for SC and CC atoms [Figs. 6(a) and 6(c)] shows a step-localized mode at 82 cm^{-1} with mainly Y and Z polarizations. This mode lies below the bulk band at 99 cm^{-1}

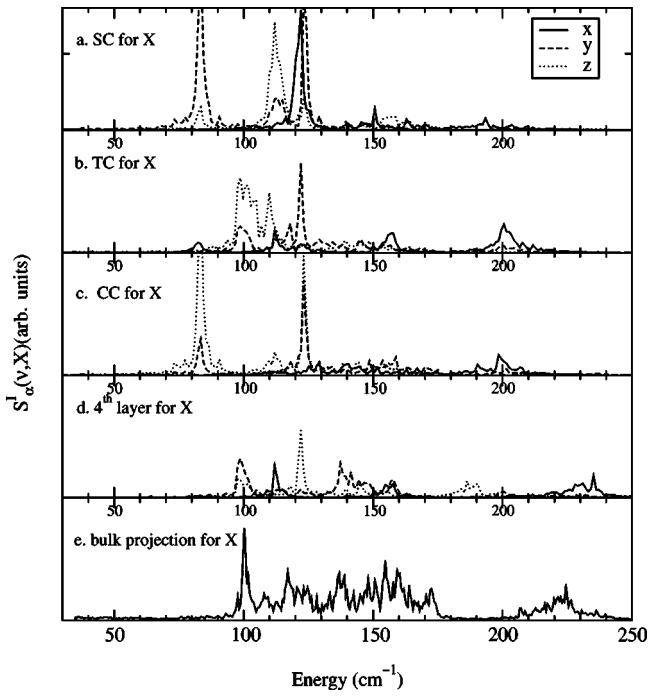

FIG. 6. PLSDP for Cu(211) surface at the $\bar{X}$ point in the reciprocal space. The bulk PLSDP corresponds to that of the 36th layer of the slab. The definition of layers is the same as in the preceding figures.

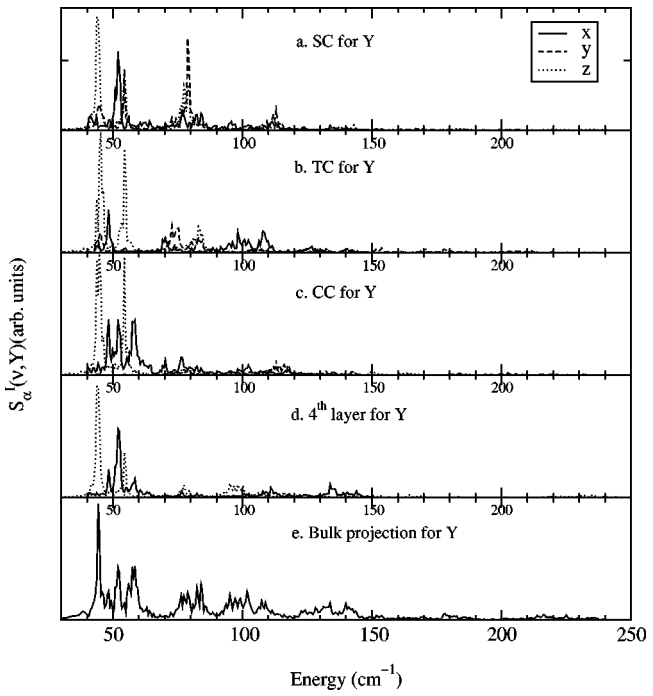

FIG. 7. PLSDP for the Cu(211) surface at the $\bar{Y}$ point in the reciprocal space.

[Fig. 6(e)]. In their HAS experiments Witte *et al.*[1] found a vibrational mode at 89.5 ± 8 cm^{-1} and suggested that this mode has a large component with polarization parallel to the surface. Extrapolating to the zone boundary the authors[1] also found a degenerated (Rayleigh and a flat step) mode with the frequency about 112.9 ± 8 cm^{-1}. In this spectral region the calculated spectra of first two layers reveal a terrace mode at 112 cm^{-1} with mainly *Z* polarization, which has a typical Rayleigh behavior. For the SC atoms we also computed a mode at 122 cm^{-1} having *X* polarization. These two modes can correspond to the experimental peak found at 112.9 ± 8 cm^{-1} but our calculation shows that they are not degenerate. In all four layers the calculated spectra show a resonance mode at 123 cm^{-1} having, respectively, *Y* polarization for SC atoms, *Y* for TC, *Y* and *Z* for CC, and *Z* for the atoms of the fourth layer. This resonance cannot be observed in the HAS experiment, which is sensitive to the *Z* motion perpendicular to the surface. For TC and CC atoms the high-energy region of the spectrum shows a surface mode at 200 cm^{-1} with an *X* polarization that can be compared with the 201 cm^{-1} peak found in the HREELS experiment[3]. Also, in agreement with the finding of HREELS,[3] the calculated spectrum displays a considerable number of lines between 100 and 125 cm^{-1}. In the fourth layer we have also computed a mode at 235 cm^{-1} [see Fig. 6(d)], which lies the maximum of the bulk frequencies. The high-frequency position of the mode is due to an increase of the force constant in Cu(211) surfaces between the first and fourth layer. Similar above bulk frequencies were also found and calculated at the $\bar{\Gamma}$ point (see discussion below and Ref. 3).

In Fig. 7 we display the calculated PLSDP spectra of the first four layers and of the bulk at the $\bar{Y}$ point of the SBZ. Analysis of these spectra shows a *Z*-polarized mode at 44 cm^{-1} interpreted as a Rayleigh mode, which appears at slightly lower frequencies down to the bulk band. For the SC atoms we found a mode with *X* polarization at 53 cm^{-1}. A resonance mode having *Y* polarization is found at 55 cm^{-1} in the spectrum of the first layer, whereas a mode at this frequency is computed for the *Z*-polarized spectra of the second and third layers. The spectrum of the SC atoms also reveals a surface localized mode at 79 cm^{-1} having *Y* and *Z* polarizations. The phonon spectra at the $\bar{Y}$ point of the reciprocal space have been measured in the HAS experiments[1] not directly but using an extrapolation procedure. For a low-frequency range Witte *et al.*[1] found a Rayleigh mode at 44.4 ± 1.6 cm^{-1}. Two modes at 61.3 ± 3.2 cm^{-1} and 84.7 ± 2.4 cm^{-1} were also observed near the $\bar{Y}$ point. Therefore, the calculated vibrational modes at 44.6 (*Z* polarized), 55 (*X* polarized), and 79 (*Y* and *Z* polarized) cm^{-1} can be compared with the peaks found in the HAS spectra at 44.4 ± 1.6, 61.3 ± 3.2, and 84.7 ± 2.4 cm^{-1}. Taking into account that the experimental results for this point of the SBZ were obtained using an extrapolation procedure and that the peak at 55 cm^{-1} has no component in *Z* polarization and therefore should be invisible in the HAS experiment, we can conclude that the agreement with experiment is excellent.

Figure 8 presents the PLSDP calculated for the $\bar{\Gamma}$ point of the SBZ. For this symmetry point the comparison of the calculated spectra can be done not only with the experimental data by Witte *et al.*[1] but also with theoretical results obtained from *ab initio* calculations by Wei *et al.*[10] and by using an EAM potential by Kara *et al.*[3]

The present MD calculations show a backfolded Rayleigh

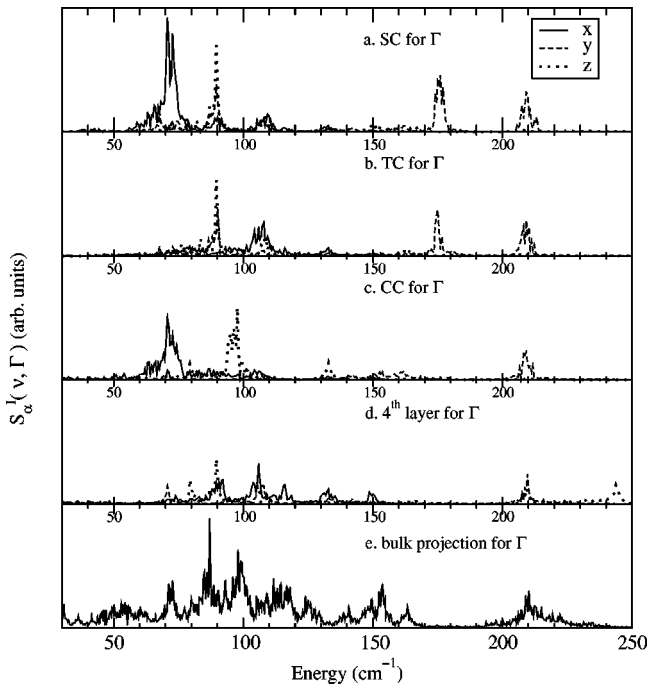

FIG. 8. PLSDP for the Cu(211) surface at the $\bar{\Gamma}$ point in the reciprocal space.

mode at 90 cm^{-1} lying in the *ZY* plane for first two layers [see Figs. 8(a) and (b)]. This result agrees with calculations by Wei and co-workers, who predicted a Rayleigh mode at 92.7 cm^{-1}, being even under reflection through the $(0\bar{1}1)$ mirror plane (*ZY* plane).[10] Witte *et al.*[1] measured a surface phonon mode at 87.9 ± 1.6 cm^{-1}. Our calculated spectra [Figs. 8(a) and 8(c)] display another peak at 74 cm^{-1}, a step mode peak characteristic for the SC and CC atoms. This peak is in qualitative agreement with a step mode that is odd under reflection through the $(0\bar{1}1)$ mirror plane calculated at 91.1 cm^{-1} by Wei *et al.*[10] Therefore, we support the assignment of Wei *et al.*[10] and found that this mode is mainly polarized in the $[0\bar{1}1]$ *X* direction. The difference in the calculated positions of this mode comes from the electronic relaxation nearby the surface step. This effect is explicitly included in the *ab initio* calculations, but ignored in the calculations using the RSC potential. As for all mainly *X* polarized modes, this mode is a poor candidate for a study using the HAS method. In summary, the low-frequency region of the PLSDP spectrum at $\bar{\Gamma}$ point is very well reproduced by our calculations.

At the high-frequency edge of the calculated PLSDP in the $\bar{\Gamma}$ point there is a resonance mode with *Y* and *Z* polarization appearing in the first four layers at 209 cm^{-1}. The mode is located just below a peak of the bulk band at 211 cm^{-1}. This feature is in a fair agreement with a peak at 210 cm^{-1} observed in the HREELS experiment[3] and with a mode at 200 cm^{-1} computed in the *ab initio* calculations.[10] Similarly to the $\bar{X}$ point of the SBZ, we find here a mode above the bulk band at a frequency of 244 cm^{-1} with *Z* polarization [see Figs. 8(d) and 8(e). Such a peak has also been measured in the HREELS experiment of Kara *et al.*[3] at around 270 cm^{-1}. Thus, the present calculations support the results of Kara *et al.*[3] that for step surfaces with (100) step facets there exists a vibrational mode above the bulk band. This mode was suggested to be due to a relaxation between first and fourth layer.[3] As mentioned above this effect is not properly taken into account by the RSC potential, which leads to computed lower frequency of the mode as compared to the other methods.

IV. DISCUSSION AND CONCLUSION

The results presented in this paper show that MD simulations using an appropriate effective interatomic potential can provide a reasonable description of the phonon spectra of stepped surfaces. In the present calculations we have used the RSC potential, which gives a phonon spectrum for flat and vicinal surfaces in good agreement with the experiments and the other theoretical calculations. We have tested the potential for the flat Cu(100) and Cu(111) surfaces and found excellent agreement for LSDP $S_\alpha(\nu)$ and PLSDP $S(\nu,\bar{k})$ with the experimental spectra for Cu(100) and Cu(111) (Refs. 33–36; Table III and Fig. 1). Due to its numerical simplicity the RSC potential is suitable for MD simulations of the dynamics for quasiperiodic systems such as surfaces for which taking a large number of elementary cells in the simulation means sampling many points in the reciprocal space. Also, the RSC potential reproduces the MSD's well for the flat and stepped surfaces. The MD method permits the calculation of the influence of the temperature on observables such as the phonon spectrum and MSD. The influence of the anharmonicity on these observables have also been discussed.

Results of the MD simulations show that for the stepped Cu(211) surface the spectra parallel to the steps (*X* direction) and perpendicular to the surface (*Z* direction) are similar to those for the flat (100) surface. The spectrum in the direction perpendicular to the step (*Y* direction) is similar to that of the flat (111) surface. In the present study a detailed analysis has been carried out for the LSDP and the PLSDP at the $\bar{\Gamma}$, $\bar{X}$, and $\bar{Y}$ points of the surface Brillouin zone. At the $\bar{\Gamma}$ reciprocal space point, the low-frequency region of the calculated PLSDP is in a good agreement with the HAS experiments (see Fig. 8), namely, we reproduce the backfolded Rayleigh mode at 90 cm^{-1}. Our calculations also reproduce a localized step mode polarized along step edges appearing at 74 cm^{-1} that cannot be seen in the HAS experiment. In the high region of the spectrum and for the fourth layer, we find a transversal mode with a frequency slightly above a cutoff frequency of the bulk spectrum. This result qualitatively agrees with HREELS experimental and EAM theoretical work of Kara *et al.*[3] The RSC semiempirical potential neglects the electronic density redistribution at the Cu(211) surface suggested by Kara *et al.*[3] to be important for this mode and therefore the agreement with their results is only qualitative. As far as we know, *ab initio* calculations for the Cu(211) phonon spectrum in the $\bar{\Gamma}$ point of the SBZ have been performed only by Wei *et al.*[10]. The agreement of the spectra computed in the present work with the results of Wei

and co-workers[10] is excellent except for the localized horizontal step mode calculated here at 74 cm^{-1} and by Wei *et al.* at 91.1 cm^{-1}. Again the discrepancy is probably due to the electronic relaxation at steps that is not properly taken into account by the RSC potential.

To our knowledge, no calculations have been reported in the literature for the surface phonon spectra at the $\overline{X}$ and $\overline{Y}$ points of the SBZ. For the $\overline{X}$ and $\overline{Y}$ points the spectra obtained here (see Figs. 6 and 7) are in fair agreement with the data of the HAS[1] and HREELS[3] experiments. For the $\overline{Y}$ point we provide evidence of a shear horizontal mode at 55 cm^{-1} polarized in the *X* direction. For the $\overline{X}$ point we suggested that degenerate Rayleigh and flat step modes observed at 112.9 ± 8 cm^{-1} in HAS are not degenerate; the Rayleigh mode is calculated here at 112 cm^{-1} and the flat step mode at 122 cm^{-1}. In the high-frequency region the calculated spectrum at the $\overline{X}$ point of the SBZ is in excellent agreement with the HREELS data of Kara *et al.*[3] As for $\overline{\Gamma}$ point, we also provide evidence of the modes lying above the bulk cutoff band due to surface relaxation.

Taking advantage of the MD method, we have followed the influence of the temperature on the phonon spectrum (see Fig. 4) and on the MSD's (see Fig. 5) of atoms. The temperature increase only slightly modifies the vibrational spectra by displacing to lower wave numbers and by broadening of the peaks. Some intensity redistribution also occurs. The MSD's reveal a roughly linear temperature dependence with a larger slope perpendicular to rather than along the steps. The difference between the harmonic approximation and MD calculation including anharmonic effects becomes significant at about 200 K or $\frac{1}{5} T_{\text{melting}}$ [taking $T_{\text{melting}} = 1350$ K for Cu (Ref. 42)]. This difference is particularly important for atoms of the first surface layer. This temperature of 200 K is higher than that obtained from the expression given by Schommers[41] for the flat Lennard-Jones surfaces.

The origin of the analytic form and parametrization of the original SC and the present RSC semiempirical potentials comes from the TB model discussed by Finnis and Sinclair[28] in their original paper. Therefore, we suggest that a more elaborate study based on a combination of TB electronic structure calculations and the molecular dynamics technique could provide better insight into the system's behavior. Particularly, such a combined method would take explicitly into account the electronic relaxation in our system and will reproduce high-energy edge dipole modes and a localized step mode at energies beyond the maximum bulk frequency. This will improve the agreement between the calculated spectrum and the results using the HREELS experiment of Kara *et al.*[3] and the *ab initio* calculations of Wei *et al.*[10]

The present RSC potential can also be used to study the adsorption at the stepped surface taking into account the energy exchange between adsorbate and surface. For example, MD simulations predicted that that a migration of the CO molecule on a rigid Cu(211) surface begins at 175 K,[43] whereas the scanning tunneling microscopy experiments showed a lower migration temperature.[44,45] It is expected that the consideration of the microscopic energy exchange between the adsorbate and the surface via surface phonons will lower the migration temperature and considerably improve the theoretical results. Other phenomena related to the adsorption and desorption processes will also be better taken into account.

TABLE IV. The experiment/calculation ratio for the elastic constants computed in the limit of large wavelengths using the RSC potential. Digits in parentheses refer to the corresponding ratio in the original paper of Sutton and Chen (Ref. 27). *L* and *T* denote longitudinal and transversal polarizations, respectively.

Direction $[n_1\, n_2\, n_3]$	$C^{L}_{n_1 n_2 n_3}$	$C^{T_1}_{n_1 n_2 n_3}$	$C^{T_2}_{n_1 n_2 n_3}$
[100]	0.96 (1.04)	1.30 (1.42)	1.30 (1.42)
[110]	1.03 (1.12)	1.30 (1.42)	1.18 (1.28)
[111]	1.06 (1.15)	1.25 (1.36)	1.25 (1.36)

ACKNOWLEDGMENTS

The authors would like to thank Dr. Pascal Parneix for very useful discussions concerning the MD method and its application.

APPENDIX: SEMIEMPIRICAL POTENTIAL RESCALED FOR THE BULK PHONON SPECTRUM OF CU

In their original paper Sutton and Chen have fitted the five parameters of the potential, Eq. (5), to the lattice constant a_0 at 0 *K* and the three elastic constants in the bulk cubic solid Cu, namely, c_{11}, c_{12}, and c_{44}.[42] However, the constraint of integer *m* and *n* ($n > m$) and of the fixed cohesive energy value E_{coh} did not permit a perfect fit of the calculated values to the experimental data.

Using the original parameters of the SC potential we have tried to reproduce the vibrational spectrum for bulk Cu and compared it with experimental[46] and previous theoretical results.[13,14,27] In our simulation of the bulk Cu we took 1500 atoms and used a slab geometry with periodic conditions in all three directions. For a quantitative comparison between results of different calculations and the experiment we have selected two peaks in the bulk phonon spectrum. The first peak corresponds to the projected longitudinal mode at the Brillouin zone boundary (ν_L) and the second one to the projected transverse mode (ν_T). Comparison between the experimental and SC frequencies in Table I shows that positions of peaks obtained with the original SC potential were shifted downwards by 10–20 %.

To improve the agreement between the experiment and the simulations we multiplied the original parameter ϵ in the SC potential by a factor 1.15 ($\epsilon_{\text{new}} = 1.15\epsilon$). The resulting potential, called below rescaled SC (RSC), yields a power spectrum in better agreement with experiment (see Table I), particularly for ν_L at the high-energy edge.

To verify that RSC gives reasonable results for other observables, we recalculated the cohesive energy E_{coh}, the elastic constants, and the elastic properties of the crystal. The energy and elastic constants are presented in the Table II and one sees that, compared to experiment, the cohesive energy

(not fixed anymore) rises by 10% and the elastic constants keep reasonable values.

Second, to calculate the elastic properties of the crystal we assume it to be a homogeneous continuous medium rather than a periodic array of atoms. Such a continuous medium model is valid for elastic waves with wavelength $\lambda \propto 10^{-6}$ cm (frequencies below 8 cm^{-1}). In cubic solids (sc, fcc, bcc) in this range of wavelengths, the dispersion relation for elastic wave in the crystallographic direction $[n_1\, n_2\, n_3]$ reads

$$ {}^{p}\omega^2_{n_1 n_2 n_3}(\vec{k}) = \frac{1}{\rho} C^{p}_{n_1 n_2 n_3} k^2, \tag{A1}$$

where ρ is the density of the solid, $k = 2\pi/\lambda$ the wave vector, $C^{p}_{n_1 n_2 n_3}$ a constant that depends on the crystallographic direction $[n_1\, n_2\, n_3]$ and p the polarization of the elastic wave. In fact, for a cubic solid the constant $C^{p}_{n_1 n_2 n_3}$ is a combination of the three elastic constants c_{11}, c_{12}, and c_{44} displayed in Table II. Table IV presents the ratio between the experimental and calculated $C^{p}_{n_1 n_2 n_3}$ constants for different directions and polarizations of the elastic wave in the Cu metal. On the average the results using the RSC potential are in better agreement with the experiment than those obtained using the original SC potential. In conclusion, the RSC potential, optimized to reproduce the phonon spectrum of bulk Cu, gives other observables in good agreement with experiment.

*Author to whom correspondence should be addressed. Electronic address: georges.raseev@ppm.u-psud.fr

[1] G. Witte, J. Braun, A. Lock, and J. P. Toennies, Phys. Rev. B **52**, 2165 (1995).
[2] L. Niu, D. D. Koleske, D. Gaspar, and S. Siebener, J. Chem. Phys. **102**, 9077 (1995).
[3] A. Kara, P. Staikov, T. S. Rahman, J. Radnik, R. Biagi, and H.-J. Erns, Phys. Rev. B **61**, 5714 (2000).
[4] R. E. Allen, G. P. Alldrege, and F. W. de Wette, Phys. Rev. B **4**, 1648 (1971).
[5] G. P. Alldrege, R. E. Allen, and F. W. de Wette, Phys. Rev. B **4**, 1666 (1971).
[6] R. E. Allen, G. Alldrege, and F. W. de Wette, Phys. Rev. B **4**, 1682 (1971).
[7] G. Armand and P. Masri, Surf. Sci. **130**, 89 (1983).
[8] J. E. Black and B. Bopp, Surf. Sci. **140**, 275 (1984).
[9] P. Knipp, Phys. Rev. B **43**, 6908 (1990).
[10] C. Y. Wei, S. P. Lewis, E. J. Mele, and A. M. Rappe, Phys. Rev. B **41**, 439 (1990).
[11] I. Y. Sklyadneva, G. G. Rusina, and E. V. Chulov, Surf. Sci. **416**, 17 (1998).
[12] S. Durukanogulu, A. Kara, and T. S. Rahman, Phys. Rev. B **53**, 15 489 (1996).
[13] S. Durukanogulu, A. Kara, and T. S. Rahnam, Phys. Rev. B **55**, 13 895 (1997).
[14] Z. J. Tian and J. E. Black, Surf. Sci. **303**, 395 (1994).
[15] A. Rahman, Phys. Rev. **136**, 405 (1964).
[16] J. P. Hansen and M. L. Klein, Phys. Rev. B **13**, 878 (1975).
[17] X. Q. Wang, L. Chiarotti, and E. Tosatti, Phys. Rev. B **38**, 8131 (1988).
[18] D. D. Koleske and S. J. Sibener, J. Electron Spectrosc. Relat. Phenom. **54/55**, 363 (1990).
[19] D. D. Koleske and S. J. Sibener, Surf. Sci. **268**, 406 (1991).
[20] D. D. Koleske and S. J. Sibener, Surf. Sci. **268**, 418 (1991).
[21] D. D. Koleske and S. J. Sibener, Surf. Sci. **290**, 179 (1993).
[22] C. Z. Wang, A. Fasolino, and E. Tosatti, Phys. Rev. B **37**, 2116 (1987).
[23] L. Yang, T. S. Rahman, and M. S. Daw, Phys. Rev. B **44**, 13 725 (1991).
[24] B. D. Todd and R. M. Lynden-Bell, Surf. Sci. **281**, 191 (1993).
[25] K. D. Hammonds and R. M. Lynden-Bell, Surf. Sci. **278**, 437 (1992).
[26] R. M. Lynden-Bell, Surf. Sci. **278**, 129 (1991).
[27] A. P. Sutton and J. Chen, Philos. Mag. Lett. **61**, 139 (1984).
[28] M. W. Finnis and J. E. Sinclair, Philos. Mag. A **50**, 45 (1984).
[29] T. Shneider and E. Stoll, Phys. Rev. B **13**, 1216 (1976).
[30] C. Z. Wang, C. T. Chan, and K. M. Ho, Phys. Rev. B **42**, 11 276 (1990).
[31] W. H. Press, S. A. Teukolsky, W. T. Vetterling, and B. P. Flannery, *Numerical Recipies in Fortran* (Cambridge, New York, 1992).
[32] M. S. Daw and M. J. Baskes, Phys. Rev. B **29**, 6443 (1987).
[33] M. Wutting, R. Franchy, and H. Ibach, Solid State Commun. **57**, 445 (1986).
[34] M. Wutting, R. Franchy, and H. Ibach, Z. Phys. B: Condens. Matter **65**, 71 (1986).
[35] B. M. Hall, D. L. Millis, M. Mohamed, and L. L. Kesmodel, Phys. Rev. B **38**, 5856 (1988).
[36] U. Harten, J. P. Toennies, and C. Woll, Faraday Discuss. Chem. Soc. **80**, 137 (1985).
[37] N. A. Levanov, V. S. Stepanyuk, W. Hergert, D. I. Bazhanov, P. H. Dederichs, A. Katsnelson, and C. Massobrio, Phys. Rev. B **61**, 2230 (2000).
[38] M. P. Allen and D. J. Tildesey, *Computer Simulation of Liquids* (Clarendon, Oxford, 1987).
[39] E. T. Chen, R R. N. Barnett, and U. Landman, Phys. Rev. B **41**, 439 (1990).
[40] H. J. C. Berendsen, J. P. M. Postma, W. F. van-Gunsteren, A. DiNola, and J. R. Haak, J. Chem. Phys. **81**, 3684 (1984).
[41] W. Schommers, *Structure and Dynamics of Surfaces* (Springer, Berlin, 1986).
[42] C. Kittel, *Introduction to Solid State Physics* (Wiley, New York, 1971).
[43] H. L. Rouzo, P. Parneix, G. Raseev, and K. Smirnov, Surf. Sci. **415**, 131 (1998).
[44] G. Meyer, S. Zophel, and K.-H. Riedel, Phys. Rev. Lett. **77**, 2113 (1996).
[45] G. Meyer, S. Zophel, and K.-H. Riedel, Phys. Rev. Lett. **78**, 1512 (1997).
[46] R. M. Nicklow, Phys. Rev. **164**, 922 (1967).
[47] G. Simmons and H. Wang, *Single Crystal Elastic Constants and Calculated Aggregated Properties* (MIT Press, Cambridge, Massachusetts, 1971).